

ARTICLES

Bonding of Benzene with Excited States of Fe₇

Israel Valencia, Victor Chávez, and Miguel Castro*

*Departamento de Física y Química Teórica, DEPg. Facultad de Química, Universidad Nacional Autónoma de México, México D. F., C. P. 04510, México**Received: December 31, 2007; Revised Manuscript Received: March 19, 2008*

The interaction between high-spin Fe₇ clusters and a benzene molecule was studied using the BPW91/6-311++G(2d,2p) method. The Fe₇–C₆H₆ ground state has a T-shaped structure, similar to that of the benzene dimer, and a multiplicity $M = 2S + 1 = 19$ (S = total spin). The carbon atoms are bonded to a single equatorial iron atom, which experiences a dramatic decrease in its magnetic moment, from 3.1 to $-0.8 \mu_B$; the magnetic moments of other Fe atoms are larger than those in the ground-state Fe₇ cluster. Such unexpected magnetic behavior of the cluster is crucial for adsorption of benzene.

1. Introduction

Nowadays, significant advances have been made in the synthesis, characterization, and understanding of small transition metal (TM) clusters.^{1,2} This has been accomplished using state-of-the-art experimental techniques for an accurate study of low-energy states of size-selected clusters. It was found that they present unexpected reactivity, magnetic, and optical properties, which strongly depend on size and, finally, on the electronic structure of the TM clusters, which is unique and different from that of the atom and bulk limits. For example, iron clusters show superparamagnetism³ and act as catalysts in the synthesis of carbon nanotubes^{4,5} and in reactions where the activation of the C–H bond is crucial.⁶ Overall, these findings open new avenues in material science, as there is the possibility of forming novel materials with specific properties using clusters as building blocks.^{7–9} But, and markedly for iron, the clusters coalesce to form bigger units when assembled.⁹ This problem can be avoided by coating the cluster with ligands, implying the study of the effects of ligands on the original attributes of the cluster. Also, a fundamental issue that is yet to be solved is the geometry of these particles. Due to their small size, insight into this property should rely on indirect methods as the chemical approach, under the assumption that cluster geometry is unaltered by the adsorbed species. However, there are limited experimental and theoretical attempts to study the effects of ligands on the behavior of clusters. For iron clusters, such studies have been done recently using small ligands such as H₂O for Fe_{*n*}, $n \leq 4$,¹⁰ C₂H₂ and CCH₂ for Fe_{*n*}, $n \leq 4$,¹¹ CH₄ for Fe_{*n*}, $n \leq 15$,^{12–14} and C₂H₆ for Fe₄.¹⁵

The objective of this work is to study interactions of benzene with a superparamagnetic Fe₇ cluster using density functional theory with generalized gradient approximation (DFT–GGA). We will specially focus on the magnetic behavior of Fe₇ upon benzene adsorption. It will be shown that the excited states of Fe₇ are more capable of adsorbing benzene than the ground state. The bonding of benzene, or its derivatives, with TM clusters may explain the origin of the existence of novel benzene–cluster

geometries.¹⁶ In advance, C₆H₆–Fe₇ has a T-shaped structure as that found for a low-lying state of the benzene dimer.

The electronic structure calculations on TM clusters pose a considerable theoretical challenge, since due to the open d-shell structure they usually have many spin states lying within a narrow energy range. Even though multireference methods, where electronic wave functions are treated as multiconfigurational functions, are more suitable and needed for the correct characterization of this kind of system, their use is limited because of their high computational cost. These methods have been only applied to the study of TM dimers¹⁷ or, regarding the present case, to the study of a TM atom interacting with a benzene moiety.¹⁸ On the other hand, DFT–GGA techniques with the use of appropriate basis sets allow the characterization of the ground-state properties for bigger clusters containing several TM atoms. Indeed, as refs 1, 2, and 5–10 show, DFT has succeeded in describing the electronic properties of magnetic TM clusters as well as the interaction of these particles with small molecules. So, a DFT-based method, described below, was chosen for the study of Fe₇–C₆H₆.

2. Methodology

The ground states (GS) of Fe₇, C₆H₆, and Fe₇–C₆H₆ were determined by means of DFT all-electron calculations, realized with the functional of Becke for exchange¹⁹ and that of Perdew and Wang for correlation.²⁰ This approach is referred to as BPW91, which is used in concert with 6-311++G(2d,2p) basis sets (15s11p6d2f)/[10s7p4d2f] for Fe, (12s6p2d)/[5s4p2d] for C, and (6s2p)/[4s2p] for H.^{21–23} The Gaussian-03 code was employed.²⁴ The BPW91/6-311++G(2d,2p) method is appropriate for the study of small iron clusters interacting with hydrocarbons.^{14,15} A strict convergence criterion was used for the total energy, minimized up to 10^{-8} au. Without imposing symmetry constraints and for several different spin states, defined by the total number of unpaired electrons, or the total spin, S , several candidate structures were fully optimized with a 10^{-5} au threshold for the rms force. An ultrafine grid was used for these steps and for the vibrational analysis, which was performed under the harmonic approximation for all the

* Corresponding author. E-mail: castro@quetzal.pquim.unam.mx.

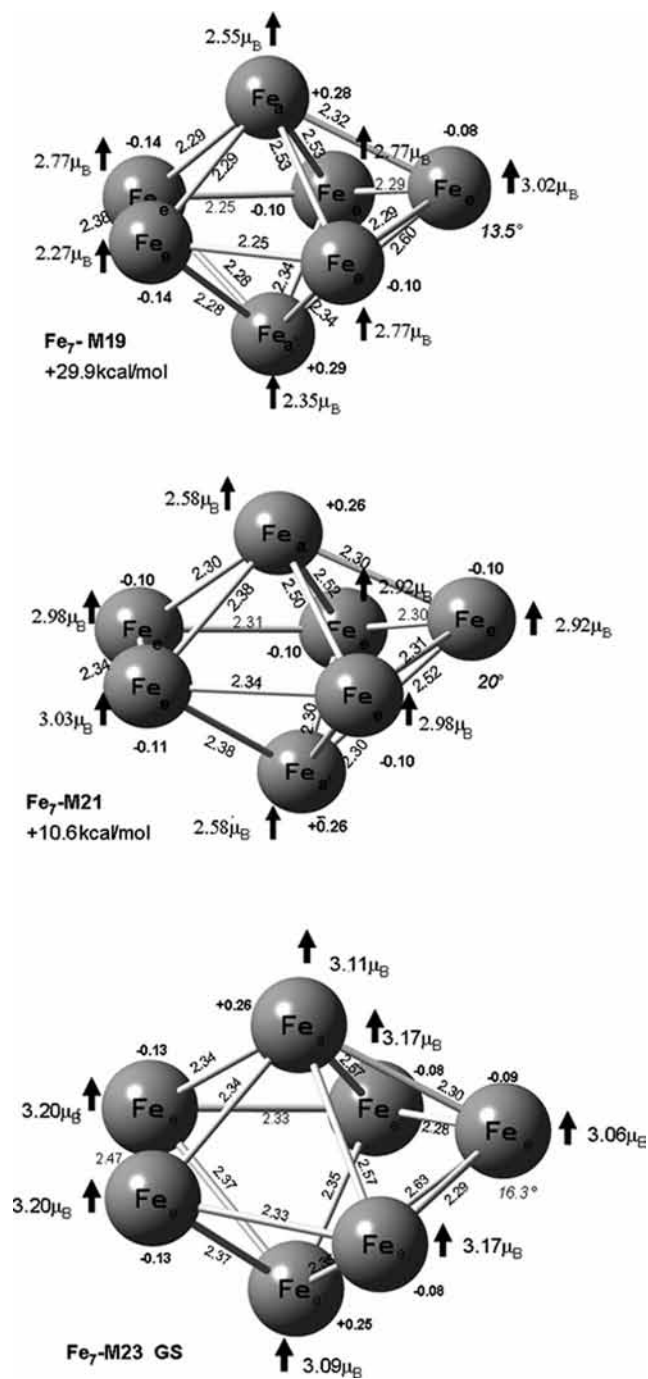


Figure 1. Bond lengths, in angstroms, atomic charges, and magnetic moments, in μ_B , for the $M = 23$, 21, and 19 states of Fe₇. Also is indicated the dihedral angle for the atom Fe_{7c}.

optimized geometries. All the located states in Figures 1 and 2 are local minima, since they have positive frequencies, on the potential energy surface. Mulliken populations were obtained to determine the magnetic moments and charge-transfer effects for the Fe₇-C₆H₆ interaction. These parameters are very useful for the analysis of the magnetic behavior of Fe₇ during the adsorption of benzene. As will be shown, the magnetic effects are crucial for the bonding of benzene with Fe₇.

3. Results and Discussion

The GS of benzene has C-C and C-H distances of 1.398 and 1.089 Å, respectively, close to the experimental values,²⁵ 1.399 and 1.101 Å; all bond angles are equal to 120°. The GS

of Fe₇ is a distorted pentagonal bipyramid, see Figure 1, with a multiplicity $M = 2S + 1 = 23$, where S is the total spin. This structure has one of the atoms of the five-membered ring located 16.3° out of the plane formed by the other four. The unpaired electrons form magnetic moments of 3.1–3.2 bohr magnetons (μ_B) at the atomic sites. The equatorial atoms have negative charges, -0.08 to -0.13 electrons (e), which are compensated by the charges, $+0.26$ e, of the axial sites. These results are in agreement with previous DFT studies.^{26,27} Furthermore, the calculated GS of Fe₇⁺ has $M = 24$ and lies 5.99 eV over the neutral GS, which is in concordance with the experimental ionization energy, 5.76 ± 0.05 eV, for Fe₇.²⁸ Similarly, addition of one extra electron yields, after full relaxation, an $M = 22$ GS for Fe₇⁻; the adiabatic electron affinity, 1.60 eV, is close to the observed value, 1.50 ± 0.05 eV.²⁹ Indeed, it is strongly believed that the GS of Fe₇ is a distorted pentagonal bipyramid with $M = 23$, as its estimated density of states²⁶ follows closely the features of the photoelectron spectrum.²⁹ However, as will be shown, the GS is not a highly reactive state. The $M = 21$ state lies 10.6 kcal/mol over the GS. Note that $M = 19$, 30 kcal/mol above the GS, is undeniably a higher energy state; its charge distribution is similar to that of the $M = 21$ and 23 states, with shorter bond lengths and smaller magnetic moments it also presents an inhomogeneous magnetization, ≈ 2.8 – $3.0 \mu_B$ at the equatorial sites and $2.55 \mu_B$ at the axial ones. At this level of theory, this $M = 19$ higher energy state presents a negative frequency, which may be due to its highly compact structure. Furthermore, since the equatorial atoms have a smaller coordination number, $NC = 4$, than the axial sites, $NC = 5$, they are more suitable for bonding with benzene, mainly those of the $M = 21$ and 19 states, as they have smaller magnetic moments (lesser amount of unpaired electrons at those sites).

The $M = 19$ excited state of Fe₇, through an equatorial atom Fe_{7c}, adsorbs benzene, forming the Fe_{7c}-C₆H₆ $M = 19$ GS (I), in which benzene and the pentagonal bipyramid lie in a T-shaped geometry similar to that of the C₆H₆ dimer,³⁰ see Figure 2. Moreover, the Fe_{7c}-C₆H₆ $M = 21$ state (II) is quasi-degenerate with the GS, since it lies less than 1.0 kcal/mol above, whereas the Fe₇ GS forms the Fe_{7c}-C₆H₆ $M = 23$ state (III), located 4.4 kcal/mol above I. Thus, the $M = 19$ and 21 Fe₇ excited states, remarkably the former, are considerably stabilized by the benzene adsorption. In fact, this process reverses the order of the magnetic states of Fe₇. Besides, carbon bonding at one axial Fe_{7a} atom yields parallel Fe₇-C₆H₆ higher energy states, considerably above the T-shaped GS.

Up to here, the spin multiplicity for the GS of the bare Fe₇ cluster was determined. As quoted, the $M = 23$ assignment is validated by the estimated ionization energy, electron affinity, and density of states, which compare well with their experimental counterparts. Moreover, the calculated spin multiplicity, $M = 19$, for the GS of Fe₇-C₆H₆ indicates a significant reduction or quenching, from 3.1 to $2.6 \mu_B$, of the average atomic magnetic moment for the coated Fe₇ cluster. Though the magnetic moment of Fe₇-C₆H₆ has not yet been reported, Knickerbein³¹ has recently found that the moments per Co atom measured for Co₇₋₁₀(C₆H₆)_m are markedly smaller than those measured for the corresponding pure Co_n clusters, clearly pointing to a strong electronic perturbation of the underlying Co_n cluster. Our spin-multiplicity assignment for Fe₇-C₆H₆ is consistent with such magnetic behavior. At low temperatures we predict an atomic moment of $2.6 \mu_B$ for Fe₇-C₆H₆, smaller than $3.1 \mu_B$ for pure Fe₇. At higher temperatures, as those reached in Stern-Gerlach experiments,³¹ 130 K, a higher magnetic moment is expected as the measurement may have

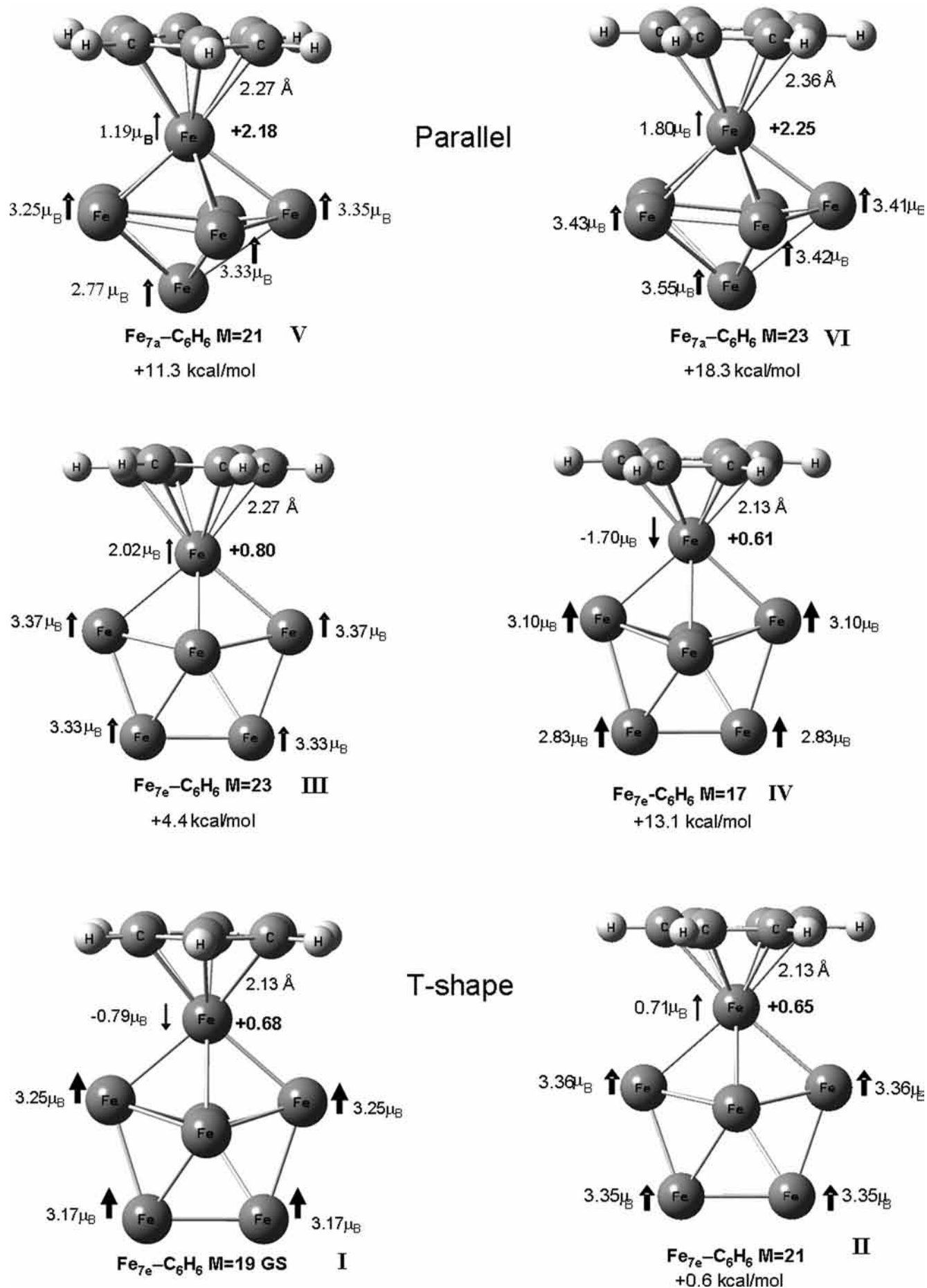


Figure 2. Bond lengths, in angstroms, atomic charges, and magnetic moments, in μ_B , for the lowest energy states of $\text{Fe}_7\text{-C}_6\text{H}_6$.

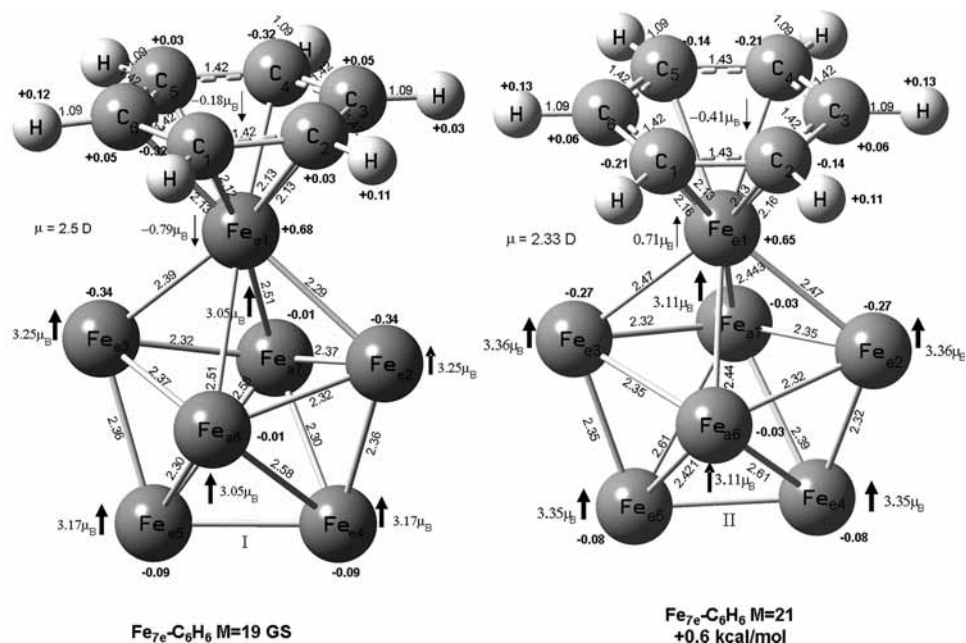


Figure 3. Bond lengths, in angstroms, atomic charges, dipole moments, in debyes, and magnetic moments, in μ_B , for the Fe_{7c}-C₆H₆ $M = 19$ GS and for **II**.

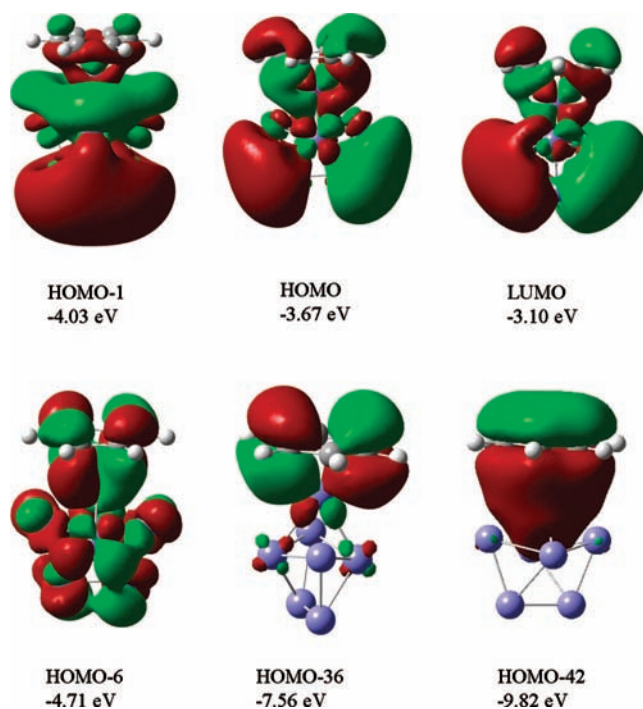


Figure 4. Contour plots for LUMO[†], HOMO[†], and other deeper MOs of **II**.

contributions from the $M = 21$ and 23 states, lying only 1 and 4 kcal/mol above the GS, respectively.

In the Fe_{7c}-C₆H₆ GS, shown in Figure 3 together with state **II**, the C-Fe_c distances, 2.116–2.129 Å, are slightly longer than those of ferrocene (2.045 Å), prototypical of C-Fe covalent bonds;³² a similar pattern holds for **II**, as its C-Fe_c lengths are 2.161–2.130 Å. For both cases, these distances are smaller than the sum of the van der Waals radii of C (1.7 Å) and Fe (1.9 Å), suggesting C-Fe bond formation; they are also shorter than the C-Fe distances, 2.253–2.381 Å, for weak C-Fe bonding in Fe₄-CH₄ and Fe₄-C₃H₈.^{14,15} As shown below, C-Fe bonds are formed in Fe₇-C₆H₆. The C-C distances in **I** (1.420–1.421 Å) or **II** (1.419–1.426 Å) show, with respect to free benzene,

a lengthening of 0.022–0.023 Å or 0.021–0.028 Å, whereas the C-H bonds, \cong 1.087 Å, have minor shrinks.

The contour plots of the highest occupied molecular orbital (HOMO), the lowest unoccupied MO (LUMO), and other deeper MOs of majority spin for **II** are shown in Figure 4. HOMO, HOMO-1, HOMO-6, and HOMO-10 have bond signatures between the 3d-electrons of Fe_{c1} and the π -cloud of C₆H₆; they also contribute largely to the other Fe atoms, for example, HOMO has large spots on Fe_{c4} and Fe_{c5} and HOMO-1 on the six Fe_{e2}-Fe_{a7} sites. These kinds of MOs show how the bonding is accomplished between Fe₇ and C₆H₆, and they also reveal a polarization from Fe_{c1} toward the other Fe sites, with an increase in their negative charge and spin density, more clearly on the

Fe sites directly bonded to Fe_{e1}. Other MOs, not shown in Figure 4, also have this type of σ -bond, formed between the π - and the 3d-electrons. Also, the LUMO presents C–Fe_e bonding, with contributions to C₆H₆ and to Fe_{e2}–Fe_{e5}. The HOMO–LUMO gap in bare benzene is 5.1 eV, and in **II** it is much smaller, 0.57 eV; because in **II**, both MOs have contributions from C₆H₆, the adsorption on Fe₇ renders a softer benzene moiety. Furthermore, HOMO-42 depicts that, aside from overlapping strongly with the electrons of Fe_{e1}, the symmetric π MO of benzene remains delocalized around the ring. A similar C–Fe_e bonding is also displayed by the MOs of **I**; the main difference is that they are located at a deeper orbital energies.

Subtracting the GS energies of Fe₇ $M = 23$ and C₆H₆ from that of Fe₇–C₆H₆ $M = 19$ GS, a binding energy (BE), including zero-point energy (ZPE), of 16.8 kcal/mol is obtained. The BE of **II** is 16.2 kcal/mol. On experimental grounds, the dissociation energy of Fe–benzene is estimated to be greater than 0.7 eV or 16.1 kcal/mol; our values are consistent with this finding for a single Fe atom^{16,33,34} and with the estimated BE of benzene, 1.07 eV or 24.67 kcal/mol, on an infinite Fe(100) surface.³⁵

From C₆H₆ to Fe₇, a small transfer of charge (0.2 e) occurs through the C–Fe_e bonds. This charge does not reside on Fe_{e1}. As indicated by the population analysis, Fe_{e1} has a charge of +0.68 e, whereas the other iron atoms have a whole negative charge of –0.90 e. The results of this strong electronic polarization of Fe₇ in **I** show how an acidic response of Fe₇ is accomplished: the (directly) bonded Fe_{e1} atom to benzene has a positive charge. Overall, this movement of charge reduces the repulsion between the “3d” electrons (mostly of majority spin in the bare cluster) localized at Fe_{e1} and the π -electrons of C₆H₆. In fact, benzene adsorption produces a dramatic decrease, and even a change of direction, of the magnetic moment at Fe_{e1}, because it is moved from 2.77 μ_B , in bare Fe₇, up to –0.79 μ_B in **I**. This decrease is compensated by the other iron atoms of the cluster, since they reach high magnetic moments (3.25 μ_B), as those of the high-spin Fe₇ $M = 23$ GS, 3.20 μ_B . Also in the opposite direction, the carbon atoms have a whole magnetic moment of –0.18 μ_B . An analogous behavior is presented by the quasi-degenerate state **II**. It has a positive charge of +0.65 e and a small magnetic moment of 0.71 μ_B at the Fe_{e1} site. In this case, four iron atoms reach magnetizations (3.36 μ_B) even greater than those of the Fe₇ $M = 23$ GS. Moreover, also the carbon atoms have a whole magnetic moment of 0.41 μ_B , but in the opposite direction. In brief, the repulsion between the Fe_{e1} 3d- and the π -electrons diminishes through a transfer of charge, associated with transference of magnetic moments, from Fe_{e1} toward the other Fe sites, leaving Fe_{e1} positively charged and with a smaller magnetic moment. These results agree with the finding that the magnetic moment of a single Fe atom is reduced from 4 to 2 μ_B when adsorbed in benzene.^{34,36} Truly, **I** and **II** have the smallest magnitudes of the magnetic moments at the Fe sites, directly bonded to the carbon atoms, than the higher energy states **III** (2.02 μ_B), **IV** (1.70 μ_B), **V** (1.19 μ_B), and **VI** (1.80 μ_B).

It should be mentioned that we have also performed geometry optimization using the smaller 6-311+G(d) basis set (15s11p6d1f)/[10s7p4d1f] for Fe, (12s6p1d)/[5s4p1d] for C, and (5s)/[3s] for H; such set has been used for the study of Fe_n interacting with NO.³⁷ The obtained results indicate a similar order for the Fe₇–C₆H₆ low-lying states. The structure **I**, Figure 2, remains as the GS, while the structures **II**, **III**, **IV**, **V**, and **VI** are located 0.9, 5.1, 13.7, 11.8, and 19.4 kcal/mol above the GS. Moreover, in **I**, the iron atom, Fe_{e1}, bonded directly to benzene, presents a magnetic moment of –0.68 μ_B , whereas in **II**, Fe_{e1} has 0.73

μ_B ; these values are close to those obtained with the 6-311++G(2d,2p) basis set.

Even more, a natural bond order³⁸ analysis also indicates a magnetic moment of –0.43 μ_B for the Fe_{e1} atom of the GS structure **I**. Similarly, a value of 0.88 μ_B was obtained for the Fe_{e1} atom of **II**. Thus, in the Fe₇–C₆H₆ GS, the magnetic moment of the Fe atom carrying the benzene molecule shows an opposite direction from that of the other Fe atoms.

The calculated 30 vibrational frequencies of free benzene fall in the 3131–394 cm^{–1} range. And those of the states **I** and **II** fall within the 3142–16 cm^{–1} and 3144–9 cm^{–1} gaps. In all cases, the upper value corresponds to the full symmetric C–H stretching, having an increase of 11 or 13 cm^{–1}. Indeed, the modes involving C–H displacements are increased from C₆H₆ to Fe₇–C₆H₆, whereas the vibrations containing C–C movements show reductions of –11 up to –111 cm^{–1}. This softening is consistent with the weakening of the C–C bonds, due to the C–Fe bonding, observed for benzene in Fe₇–C₆H₆.

4. Conclusions

The $M = 19$ and 21 excited states of Fe₇ adsorb benzene forming the lowest energy states of Fe₇–C₆H₆ with a T-shaped geometry and with the carbon atoms bonded to a single Fe_{e1} atom. However, the Fe₇–C₆H₆ $M = 23$ state lies only 4.4 kcal/mol over the $M = 19$ GS. Thus, in these coated Fe₇ clusters the $M = 23$ –19 magnetic states are contained within a gap of 4.4 kcal/mol, indicating a significant decrease from that, 30 kcal/mol, of the free clusters. These results show how the magnetic effects play a crucial role in the absorption of C₆H₆ by Fe₇. This process produces a strong polarization on Fe₇, yielding a positive charge, +0.65 or +0.68 e, and a severe reduction of the magnetic moment, 0.7 or 0.8 μ_B , at the iron atom, Fe_{e1}, bonded directly with the carbon atoms, whereas other iron atoms have an increase of charge and of magnetic moments. Such charge and magnetic polarization reduces the repulsion between the 3d-electrons of Fe_{e1} and the π -electrons of benzene, facilitating the Fe₇–C₆H₆ bonding through an acid behavior of Fe₇ and through C–Fe σ bond formation.

Acknowledgment. Financial support from Project PAPIIT IN-107905 from DGAPA-UNAM is acknowledged. The access to the supercomputer facilities at DGSCA-UNAM is strongly appreciated.

References and Notes

- (1) Bansmann, J. *Surf. Sci. Rep.* **2005**, *56*, 189.
- (2) Alonso, J. A. *Chem. Rev.* **2000**, *100*, 637.
- (3) Khanna, S. N.; Linderth, S. *Phys. Rev. Lett.* **1991**, *67*, 742.
- (4) Nikolaev, P.; Bronikowski, M. J.; Bradley, R. K.; Rohmund, F.; Colbert, D. T.; Smith, K. A.; Smalley, R. E. *Chem. Phys. Lett.* **1999**, *313*, 91.
- (5) Satishkumar, B. C.; Govindaraj, A.; Sen, R.; Rao, C. N. R. *Chem. Phys. Lett.* **1998**, *293*, 47.
- (6) Schnabel, P.; Irion, M. P.; Weil, K. G. *J. Phys. Chem.* **1991**, *95*, 9688.
- (7) Eberhardt, W. *Surf. Sci.* **2002**, *500*, 242.
- (8) Chen, B.; Castlemann, A. W., Jr.; Ashman, C.; Khanna, S. N. *Int. J. Mass Spectrom.* **2002**, *220*, 171.
- (9) Vystavel, T.; Koch, S. A.; Palasantzas, G.; De Hosson, J. Th. M. *J. Mater. Res.* **2005**, *20*, 1785.
- (10) Gutsev, G. L.; Mochena, M. D.; Bauchlicher, C. W., Jr. *Chem. Phys.* **2005**, *314*, 291.
- (11) Chrétien, S.; Salahub, D. R. *J. Chem. Phys.* **2003**, *119*, 12279.
- (12) Liyanage, R.; Zhang, X.-G.; Armentrout, P. B. *J. Chem. Phys.* **2001**, *115*, 9747.
- (13) (a) Chiodo, S.; Kondakova, O.; Michelini, M. C.; Russo, N.; Sicilia, E.; Irgoras, A.; Ugalde, J. M. *J. Phys. Chem. A* **2004**, *108*, 1077. (b) Chiodo, S.; Rivalta, I.; Michelini, M. C.; Russo, N.; Sicilia, E.; Ugalde, J. M. *J. Phys. Chem. A* **2004**, *110*, 12501.

- (14) Castro, M. *Chem. Phys. Lett.* **2007**, *435*, 322.
(15) Castro, M. *Chem. Phys. Lett.* **2007**, *446*, 333.
(16) Kurikawa, T.; Takeda, H.; Hirano, M.; Judai, K.; Arita, T.; Nagano, S.; Nakajima, A.; Kaya, K. *Organometallics* **1999**, *18*, 1430.
(17) Hübner, O.; Sauer, J. *Chem. Phys. Lett.* **2002**, *358*, 442.
(18) Rabilloud, F. *J. Chem. Phys.* **2005**, *122*, 134303.
(19) Becke, A. D. *Phys. Rev. A* **1988**, *38*, 3098.
(20) Perdew, J. P.; Wang, Y. *Phys. Rev.* **1992**, *45*, 13244.
(21) Wachters, A. J. H. *J. Chem. Phys.* **1970**, *52*, 1033.
(22) Hay, P. J. *J. Chem. Phys.* **1977**, *66*, 4377.
(23) Raghavachari, K.; Trucks, G. W. *J. Chem. Phys.* **1989**, *91*, 1062.
(24) Frisch, M. J.; Trucks, G. W.; Schlegel, H. B.; Scuseria, G. E.; Robb, M. A.; Cheeseman, J. R.; Montgomery, J. A., Jr.; Vreven, T.; Kudin, K. N.; Burant, J. C.; Millam, J. M.; Iyengar, S. S.; Tomasi, J.; Barone, V.; Mennucci, B.; Cossi, M.; Scalmani, G.; Rega, N.; Petersson, G. A.; Nakatsuji, H.; Hada, M.; Ehara, M.; Toyota, K.; Fukuda, R.; Hasegawa, J.; Ishida, M.; Nakajima, T.; Honda, Y.; Kitao, O.; Nakai, H.; Klene, M.; Li, X.; Knox, J. E.; Hratchian, H. P.; Cross, J. B.; Bakken, V.; Adamo, C.; Jaramillo, J.; Gomperts, R.; Stratmann, R. E.; Yazyev, O.; Austin, A. J.; Cammi, R.; Pomelli, C.; Ochterski, J. W.; Ayala, P. Y.; Morokuma, K.; Voth, G. A.; Salvador, P.; Dannenberg, J. J.; Zakrzewski, V. G.; Dapprich, S.; Daniels, A. D.; Strain, M. C.; Farkas, O.; Malick, D. K.; Rabuck, A. D.; Raghavachari, K.; Foresman, J. B.; Ortiz, J. V.; Cui, Q.; Baboul, A. G.; Clifford, S.; Cioslowski, J.; Stefanov, B. B.; Liu, G.; Liashenko, A.; Piskorz, P.; Komaromi, I.; Martin, R. L.; Fox, D. J.; Keith, T.; Al-Laham, M. A.; Peng, C. Y.; Nanayakkara, A.; Challacombe, M.; Gill, P. M. W.; Johnson, B.; Chen, W.; Wong, M. W.; Gonzalez, C.; Pople, J. A. *Gaussian 03*, revision D.01; Gaussian, Inc.: Wallingford, CT, 2004.
- (25) Kuchitsu, K. *Structure Data of Free Polyatomic Molecules*; Landolt-Börnstein, New Series, Group II; Springer: Heidelberg, 1992; Vol. 21.
(26) Castro, M. *Int. J. Quantum Chem.* **1997**, *64*, 223.
(27) Bobadova-Parvanova, P.; Jackson, K. A.; Srinivas, S.; Horoi, M.; Kohler, C.; Seifert, G. *J. Chem. Phys.* **2002**, *116*, 3576.
(28) Yand, S.; Knickelbein, M. B. *J. Chem. Phys.* **1990**, *93*, 1533.
(29) Wang, L.-S.; Li, X.; Zhang, H.-F. *Chem. Phys.* **2000**, *262*, 53.
(30) Sinnokrot, M. O.; Valeev, E. F.; Sherill, C. D. *J. Am. Chem. Soc.* **2002**, *124*, 10887.
(31) Knickelbein, M. B. *J. Chem. Phys.* **2006**, *125*, 044308.
(32) (a) Wilkinson, G.; Rosenblum, M.; Whiting, M. C.; Woodward, R. B. *J. Am. Chem. Soc.* **1952**, *74*, 2125. (b) Dunitz, J. D.; Orgel, L. E.; Rich, A. *Acta Crystallogr.* **1956**, *9*, 373.
(33) Mayer, F.; Khan, I. A.; Armentrout, P. B. *J. Am. Chem. Soc.* **1995**, *117*, 9740.
(34) Pandey, R.; Rao, B. K.; Jena, P.; Newsam, J. M. *Chem. Phys. Lett.* **2000**, *321*, 142.
(35) Sun, X.; Suzuki, T.; Kurashashi, M.; Shang, J. W.; Yamauchi, Y. *J. Appl. Phys.* **2007**, *101*, 09G256.
(36) Pandey, R.; Rao, B. K.; Jena, P.; Blanco, M. A. *J. Am. Chem. Soc.* **2001**, *123*, 3799.
(37) Gutsev, G. L.; Mochena, M. D.; Johnson, E.; Bauchlicher, C. W., Jr. *J. Chem. Phys.* **2006**, *125*, 194312.
(38) Reed, A. E.; Curtiss, L. A.; Weinhold, F. *Chem. Rev. (Washington, DC, U.S.)* **1988**, *88*, 899.

JP712184W